



1998

Atomic and electronic structure of neutral and charged SinOm clusters

Saroj K. Nayak

Virginia Commonwealth University

B. K. Rao

Virginia Commonwealth University

S. N. Khanna

Virginia Commonwealth University, snkhanna@vcu.edu

P. Jena

Virginia Commonwealth University, pjena@vcu.edu

Follow this and additional works at: http://scholarscompass.vcu.edu/phys_pubs

 Part of the [Physics Commons](#)

Nayak, S. K., Rao, B. K., & Khanna, S. N., et al. Atomic and electronic structure of neutral and charged SinOm clusters. *The Journal of Chemical Physics*, 109, 1245 (1998). Copyright © 1998 American Institute of Physics.

Downloaded from

http://scholarscompass.vcu.edu/phys_pubs/143

This Article is brought to you for free and open access by the Dept. of Physics at VCU Scholars Compass. It has been accepted for inclusion in Physics Publications by an authorized administrator of VCU Scholars Compass. For more information, please contact libcompass@vcu.edu.

Atomic and electronic structure of neutral and charged Si_nO_m clusters

S. K. Nayak, B. K. Rao, S. N. Khanna, and P. Jena

Physics Department, Virginia Commonwealth University, Richmond, Virginia 23284-2000

(Received 24 November 1997; accepted 16 April 1998)

Using molecular orbital approach and the generalized gradient approximation in the density functional theory, we have calculated the equilibrium geometries, binding energies, ionization potentials, and vertical and adiabatic electron affinities of Si_nO_m clusters ($n \leq 6, m \leq 12$). The calculations were carried out using both Gaussian and numerical form for the atomic basis functions. Both procedures yield very similar results. The bonding in Si_nO_m clusters is characterized by a significant charge transfer between the Si and O atoms and is stronger than in conventional semiconductor clusters. The bond distances are much less sensitive to cluster size than seen for metallic clusters. Similarly, calculated energy gaps between the highest occupied and lowest unoccupied molecular orbital (HOMO-LUMO) of $(\text{SiO}_2)_n$ clusters increase with size while the reverse is the norm in most clusters. The HOMO-LUMO gap decreases as the oxygen content of a Si_nO_m cluster is lowered eventually approaching the visible range. The photoluminescence and strong size dependence of optical properties of small silica clusters could thus be attributed to oxygen defects. © 1998 American Institute of Physics. [S0021-9606(98)01528-1]

I. INTRODUCTION

Silica is one of the most abundant material on earth.¹ Its importance in science and technology results from its diverse use ranging from glass to catalysis to Si-based microelectronic devices² and optical fiber communications.³ It is, therefore, not surprising that considerable efforts have been made in the past to understand the structural, optical and electronic properties of bulk silica in crystalline and amorphous phase.⁴ However, interest in studying the properties of nanoparticles and clusters of silica is relatively recent.⁵⁻⁷ In view of the fact that materials at the nanoscale possess novel properties and silica is a technologically important material, a fundamental understanding of the structure, bonding, stability, and properties of silica clusters and nanoparticles is important.⁸

In a recent experiment on laser induced vaporization of polycrystalline silicon in rare gas and oxygen environment, El-Shall *et al.*⁶ have observed a weblike form of nanostructured silica exhibiting bright blue photoluminescence. While the origin of this photoluminescence is not yet completely clarified, the authors proposed that this could be due to large concentration of Si(II) type defects. Whether the photoluminescence of nanoparticles of silica could equally arise from the effect of size on the energy gap between the highest occupied molecular orbital (HOMO) and lowest unoccupied molecular orbital (LUMO) has not been explored to our knowledge.

Recently Harkless *et al.*⁷ have calculated the structures and energies of $(\text{SiO}_2)_n$ clusters ($1 \leq n \leq 8$ and $n=18$) using the molecular dynamics simulation and an empirical pairwise interatomic potential originally developed for simulation studies of crystalline and amorphous condensed phases of silica. In addition to the obvious concern that such potentials may not be applicable for studies of small clusters, classical molecular dynamics simulation does not provide any elec-

tronic structure information. The only experimental work that has been targeted toward achieving an atomic level understanding of the oxidation process of silicon through studies of Si_nO_m clusters is due to Wang *et al.*^{5,9} These authors have carried out photoelectron spectroscopy experiments on size selected Si_3O_m ($m=1-6$) clusters to obtain information on electronic structure. They also carried out parallel theoretical calculations of the geometries, adiabatic, and vertical ionization potentials for these clusters using the molecular orbital (MO) technique, Gaussian basis sets for the atomic functions, and Hartree-Fock second order Moller-Plesset perturbation theory (MP2) for exchange and correlation contribution to the energy. Core electrons were frozen in all MP2 calculations.

In this paper we present a systematic study of the equilibrium geometries, binding energies, HOMO-LUMO gap, and vertical and adiabatic electron affinities of Si_3O_m ($m=1,4,6$) using density functional theory. Contrary to the results of Fan *et al.*,⁹ we find that the results of the density functional theory agree very well with those obtained using MP2 formalism and with experiment. In addition, we also present results on $(\text{SiO}_2)_n$ clusters for $1 \leq n \leq 6$. In Sec. II, we provide a brief description of our theoretical procedure. Our results are discussed in Sec. III followed by a summary of our conclusions in Sec. IV.

II. COMPUTATIONAL METHODS

Our calculations are based on the self-consistent field linear combination of atomic orbitals-molecular orbital (SCF-LCAO-MO) theory. The total energies, equilibrium geometries, and electronic structure are computed using density functional theory. The exchange-correlation contribution to the total energy was treated at the generalized gradient approximation (GGA) level of theory using Perdew-Wang expression for exchange¹⁰ and the Becke form for

correlation.¹¹ The atomic basis functions were also treated in two different ways—the Gaussian-type functions and numerical functions. For the former, we have used GAUSSIAN 94 software¹² (with 6-311G** basis functions), while for the later we have used the DMOL software¹³ with double numerical basis functions with polarization function (DNP). The Gaussian calculations were carried out at the all-electron level, while in DMOL the inner core of the atoms were frozen. We have verified that the frozen core potential yields results in excellent agreement with all electron results in the GAUSSIAN 94 code. We used two independent numerical methods since Fan *et al.*⁹ had noted that the density functional theory was inadequate to explain the results of Si₃O₄ cluster. We wanted to examine if the difficulty lies with the numerical procedure or with the density functional theory.

To examine the numerical accuracy of our procedure, we have first calculated the equilibrium geometries, binding energies, ionization potentials, and electron affinities of SiO and Si₃O_m ($m=1,4,6$) clusters and compare these with experiment and previous MP2 calculations.^{5,9} The equilibrium geometries of these clusters and Mulliken charges on Si and O atoms calculated using GAUSSIAN 94 software (DFT-GGA) and DMOL are given in Fig. 1(a). The corresponding bond lengths are given in Table I and compared with earlier calculations based on MP2 theory.^{5,9} Identical geometries were obtained using the DMOL software. These geometries also agree very well with those computed earlier by Wang *et al.*^{5,9} using the MP2 level of theory. We note that oxygen prefers to have two nearest neighbor Si atoms while Si prefers to be four-fold coordinated with oxygen if permitted by the stoichiometry of the cluster. In addition, the SiO bond length when O is two-fold coordinated with Si remains essentially unchanged with increasing cluster size. There is transfer of charge from Si to O atoms and the Mulliken charges on various atoms are also insensitive to cluster size. These results indicate that the bonding characteristics of these clusters have evolved to almost bulklike behavior even for the smallest clusters.

In Fig. 1(b) we give the geometries of the Si₃O_m⁻ ($m=1,4,6$) clusters. While the geometries of the anions remain similar to those of neutral clusters, the bond lengths especially in Si₃O₄⁻ and Si₃O₆⁻ do differ from the neutral clusters. More importantly, the Mulliken charge distribution in anionic clusters differs substantially from those in the neutral clusters. For example, in Si₃O⁻ almost as much negative charge resides on one of the Si atoms as on the oxygen atom. On the other hand, in Si₃O₄⁻ and Si₃O₆⁻ clusters, no Si atom carries a negative charge.

In Table II we compare the binding energies, ionization potentials, and electron affinities calculated using GAUSSIAN 94 and DMOL codes with available experimental and MP2 results.^{5,9} For SiO both theories yield binding energies in good agreement with experiment. The vertical and adiabatic electron affinities agree very well with both MP2 and experimental results. There are no measured vertical ionization potentials of Si₃O_m ($m=1,4,6$), but our value for SiO again agrees very well with experiment.¹⁵ Thus we conclude that the density functional theory at the GGA level can provide reliable results. We have also repeated the vertical and adia-

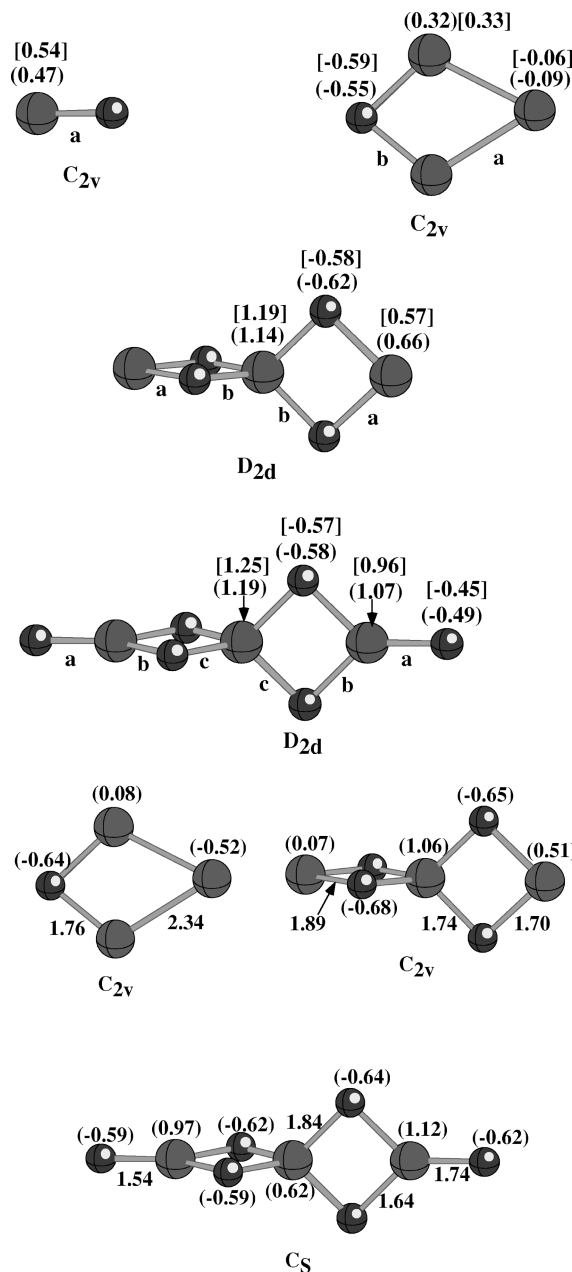


FIG. 1. (a) Equilibrium geometries of neutral SiO, Si₃O_m ($m=1,4,6$) clusters using GAUSSIAN 94 and DMOL codes. Small dark balls represent O atom and large gray balls represent Si atom. Corresponding bond lengths indicated in the figures are given in Table I. Mulliken charges on various atoms are shown in the figure; values given in () are obtained from GAUSSIAN 94 calculation and [] values are from DMOL code. (b) Equilibrium geometries of Si₃O_m⁻ ($m=1,4,6$) clusters. Bond lengths (Å) and Mulliken charge distribution shown in the figure are obtained from GAUSSIAN 94 code.

batic electron affinity calculations of Si₃O₄ using the Vosko-Wills-Nusair form¹⁴ for the local density approximation (LDA) in the GAUSSIAN 94 code. These results are 1.12 eV and 0.67, respectively, which also agree well with the experimental values in Table II. While this comparison might indicate that LDA may be just as good as GGA level of theory, we have carried out the remaining calculations using the GGA.

TABLE I. Comparison of bond lengths in SiO and Si₃O_m (*m* = 1,4,6) clusters obtained using various theoretical approaches.

Cluster	Method	Bond lengths (Å)		
		a	b	c
SiO	GAUSSIAN 94	1.54		
	DMOL			
	MP2 (Ref. 5)			
Si ₃ O	GAUSSIAN 94	2.31	1.74	
	DMOL	2.31	1.75	
	MP2 (Ref. 5)	2.30	1.75	
Si ₃ O ₄	GAUSSIAN 94	1.74	1.69	
	DMOL	1.75	1.68	
	MP2 (Ref. 5)	1.72	1.67	
Si ₃ O ₆	GAUSSIAN 94	1.53	1.70	1.70
	DMOL	1.54	1.71	1.69
	MP2 (Ref. 5)	1.53	1.69	1.68

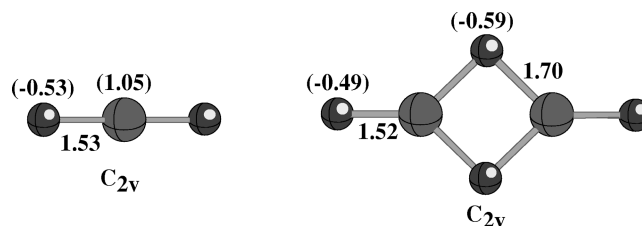
III. RESULTS AND DISCUSSIONS ON (SiO₂)_N CLUSTERS

Harkless *et al.*⁷ have employed extensive configurational searches to locate the global equilibrium geometries as well as of isomers of (SiO₂)_n (*n* ≤ 8) clusters using an additive pair interaction potentials developed by Tsuneyuki *et al.*¹⁶ The authors found that the stable clusters of SiO₂ do not resemble any of the known crystalline SiO₂ polymorphs. Since these potentials were developed for bulk systems and lack directional dependence, we have calculated the equilibrium geometries of the ground state and higher energy isomers using the GAUSSIAN 94 and the GGA level of theory. We have optimized several structural forms in order to obtain the lowest energy structures.

We begin with the geometry of SiO₂ cluster (see Fig. 2). Analogous to the CO₂ molecule, the geometry of SiO₂ is linear with an Si–O bond length of 1.53 Å and a binding

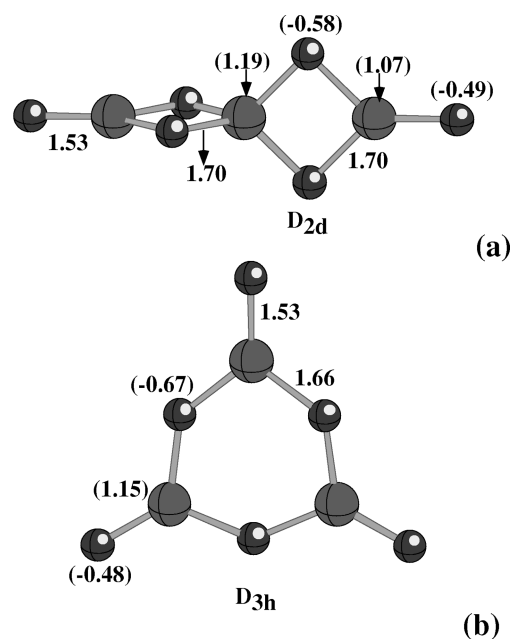
TABLE II. Comparison of calculated binding energies (measured against dissociated atoms), vertical ionization potentials, and adiabatic electron affinities of Si_nO_m clusters with experiments and previous calculations.

Computed quantity	Method of calculation	Clusters			
		SiO	Si ₃ O	Si ₃ O ₄	Si ₃ O ₆
Binding energy (eV)	GAUSSIAN 94	8.06	13.79	34.85	45.30
	DMOL	8.49	14.61	36.84	48.12
	Expt. (Ref. 9)	8.26			
Vertical ionization potential (eV)	GAUSSIAN 94	11.27	8.13	9.47	13.71
	DMOL	11.44	8.15	9.62	11.02
	Expt. (Ref. 9)	11.43			
Vertical electron affinity (eV)	GAUSSIAN 94		1.78	1.20	3.65
	DMOL		1.86	1.30	3.80
	MP2 (Ref. 8)		1.84	1.10	3.68
Adiabatic electron affinity (eV)	Expt. (Ref. 9)		1.96	1.05	> 3.50
	GAUSSIAN 94		1.69	0.70	2.25
	DMOL		1.78	0.83	2.46
Adiabatic electron affinity (eV)	MP2 (Ref. 5)		1.74	0.57	2.09
	Expt. (Ref. 9)		1.76	0.46	< 3.10

FIG. 2. Equilibrium structures of SiO₂ and (SiO₂)₂.

energy of 8.06 eV. We define the binding energy as the energy necessary to dissociate the cluster into separated atoms. While our calculated bond length is reasonably close to the 1.46 Å value obtained by Harkless *et al.*,⁷ our binding energy differs substantially from their value of 44.73 eV. The Mulliken charge on the Si and O atoms are indicated in parentheses in Fig. 2. A net charge of +1.05 on Si and -0.53 on O is indicative of partial ionic bonding in SiO₂.

This trend continues as SiO₂ clusters grow. The ground state geometry of (SiO₂)₂ in Fig. 2 has a planar C_{2v} structure with ¹A₁ electronic state. The O atoms form a symmetric structure. The bond length between Si and O atoms forming a double bridge between Si atoms is elongated compared to the bond between the external O atom with Si. As we will see in the following this trend continues as trimers and higher clusters of SiO₂ form. The charge on the O atoms and Si atoms remain fairly close to their value in the SiO₂ monomer. This indicates that partial ionic bonding continues with increasing silica cluster size. This is in contrast to clusters of CO₂. For example, the binding in (CO₂)₂ is of weak van der Waals character. The binding energy of the (SiO₂)₂ dimer against the separated SiO₂ monomer is 3.67 eV which again differs significantly from the empirical potential calculation of Harkless *et al.* (5.35 eV).⁷

FIG. 3. Geometries of (SiO₂)₃ cluster corresponding to the ground state and two higher energy configurations.

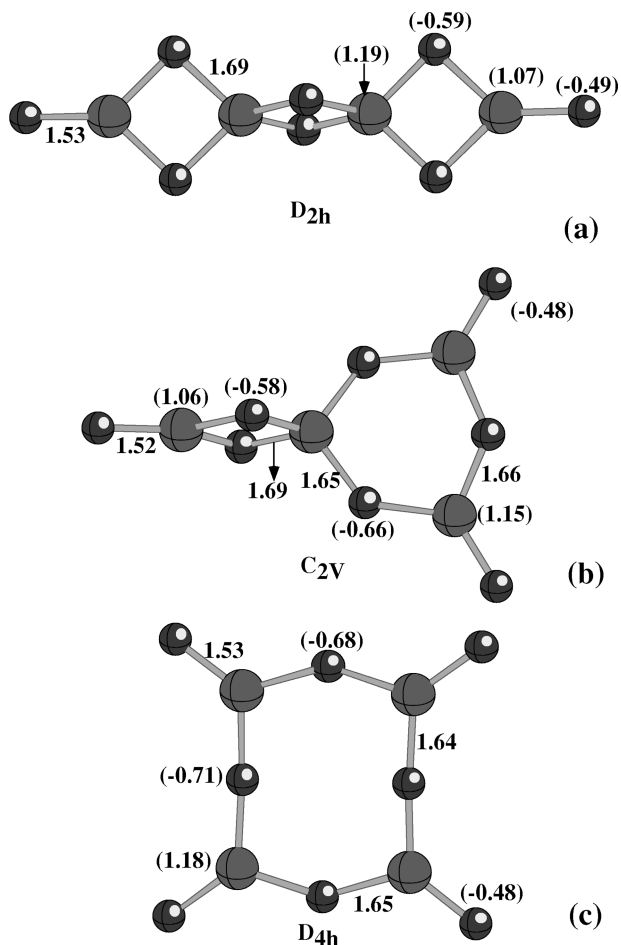


FIG. 4. Ground state geometry and the next higher energy isomers of $(\text{SiO}_2)_4$ clusters. See the text for details.

The geometries of the $(\text{SiO}_2)_3$ isomers are shown in Fig. 3. Harkless *et al.*⁷ have identified two structures of $(\text{SiO}_2)_3$: a planar ring structure with D_{3h} symmetry and a three-dimensional structure with D_{2d} symmetry where four O atoms belong to double bridges and two end O atoms bonded to Si atoms. The authors found the D_{3h} structure to be lower in energy from the D_{2d} structure by 0.43 eV. Our results are just the opposite. We find the D_{2d} structure to be the ground state which lies 0.69 eV lower in energy from the D_{3h} structure. This can be explained by examining the coordination of the individual Si and O atoms. We note that Si is tetravalent and O is divalent. Thus ideally in a given cluster structure, Si and O would, respectively, prefer to be four-fold and two-fold coordinated. This is what we noted in the structures in Fig. 1. In Fig. 3(a) one Si atom is four-fold coordinated and four O atoms are two-fold coordinated while in Fig. 3(b) no Si and only three O atoms satisfy the above bonding preference. Consequently the structure of Fig. 3(a) is more stable than that in Fig. 3(b). Our calculations confirm this. It is worth noting that the bond lengths between double bridging O and Si as well as the external Si–O bond lengths compare well with the data obtained from the empirical potential.⁷ This suggests that while the empirical potential does not yield the relative stabilities of silica cluster isomers correctly, it reproduces the bond lengths accurately.

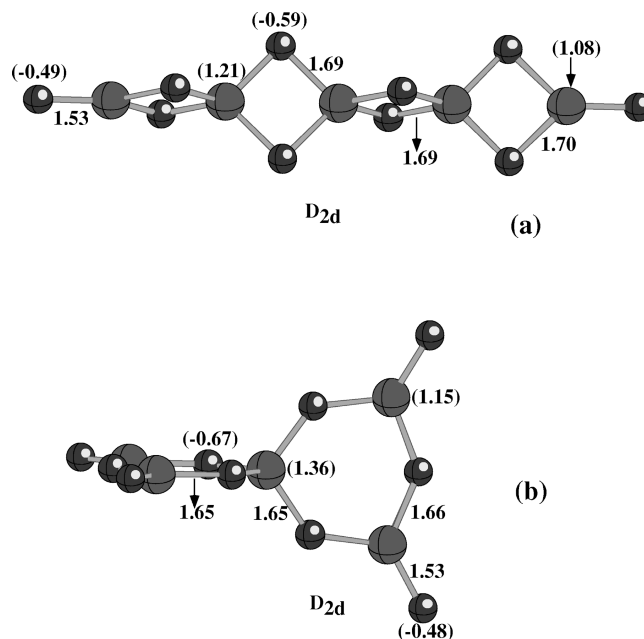


FIG. 5. Lowest energy structure and the higher energy geometry for $(\text{SiO}_2)_5$ cluster.

The ground state of the silica tetramer $(\text{SiO}_2)_4$ given in Fig. 4(a) is simply an extension of the trimer structure. This arises as the SiO_2 unit attaches to the end O atom of the $(\text{SiO}_2)_3$ and two O atoms take part in forming double bridges. We have identified two other isomers of $(\text{SiO}_2)_4$ which have C_{2v} and D_{4h} (see Fig. 4) symmetry. These structures labeled (b) and (c) are 0.53 eV and 2.24 eV above the ground state structure [Fig. 4(a)], respectively. As mentioned in the previous paragraph, the relative stability of these isomers can be predicted from counting the coordination numbers of each of the Si and O atoms in Fig. 4. In Fig. 4(a) two Si and six O atoms have the preferred four-fold and two-fold coordination, respectively, while in Fig. 4(b) only one Si and five O atoms have this desired coordination. In Fig. 4(b) none of the Si atoms and four of the O atoms have the desired coordination. This bonding analysis is consistent with the relative energies of the structures in Fig. 4. It is important to realize that the nature of bonding remains similar to that of the smaller clusters as can be seen from the similarity of the bond lengths and Mulliken charge distribution.

The ground state of $(\text{SiO}_2)_5$ is shown in Fig. 5(a). The structure is again an extension of the preceding tetramer cluster. Although we have carried out structural optimization without any symmetry constraint, the optimized structure was found to have a D_{2d} symmetry. It should be pointed out that Harkless *et al.*⁷ had obtained a different three-dimensional structure [Fig. 5(b)] as the ground state geometry. We have calculated the total energy for this structure by optimizing all the bond lengths and bond angles and have found that it is 1.03 eV higher in energy compared to the structure in Fig. 5(a). Similarly, the lowest energy structure of $(\text{SiO}_2)_6$ is the result of addition of a SiO_2 unit to the pentamer structure and is shown in Fig. 6(a). The other three dimensional structure [see Fig. 6(b)] which was identified by Harkless *et al.*⁷ as the ground state indeed lies 0.98 eV

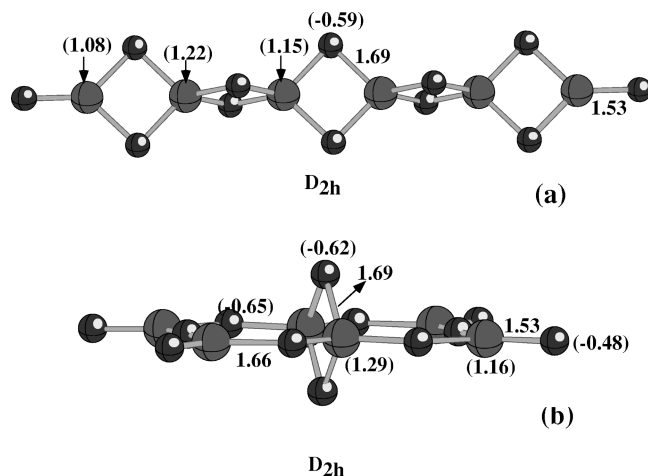


FIG. 6. Lowest energy structure and the higher energy isomer for $(\text{SiO}_2)_6$ cluster.

higher in energy compared to the structure in Fig. 6(a). We once again note that the structure in Fig. 6(a) has more Si and O atoms that have their ideal coordination numbers than those in Fig. 6(b). It is also to be noted here that the SiO bond lengths for double bridging O atoms remain the same as in smaller clusters. The Mulliken charge on interior Si atoms also remain invariant.

In Table III, we present the binding energies of the $(\text{SiO}_2)_n$ clusters calculated using both GAUSSIAN 94 and DMOL software. The binding energy is defined as,

$$E_b = E(\text{Si}_n\text{O}_m) - nE(\text{Si}) - mE(\text{O}), \quad (3.1)$$

where E is the total energy of the cluster or atom as indicated. Note that the calculated binding energies agree very well with each other. For larger clusters $(\text{SiO}_2)_n (n \geq 5)$, we have only carried out Gaussian orbital based studies.

The relative stabilities of these clusters can be better understood by calculating the energy gained by adding successive monomers (SiO_2 units) to silica clusters. We define $\Delta E(n)$, the energy gain in adding a (SiO_2) monomer to $(\text{SiO}_2)_n$ cluster, as

$$\Delta E(n) = -E(n+1) + E(n), \quad n \geq 1. \quad (3.2)$$

In Fig. 7 we plot $\Delta E(n)$ as a function of n . Note that the energy gain in adding a SiO_2 to a silica cluster abruptly increases from $n=1$ to $n=2$, but then remains essentially constant as the clusters grow. Except for this sharp increase,

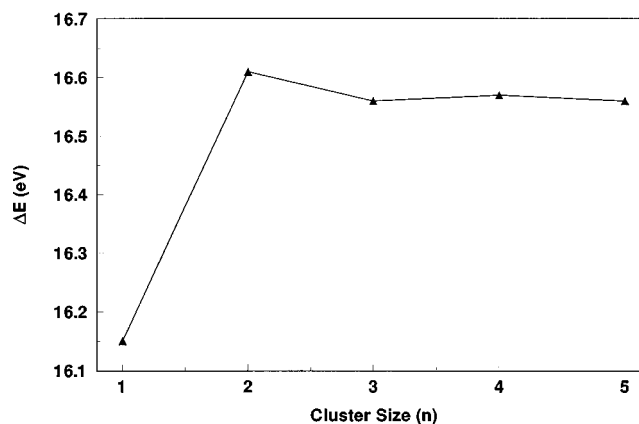


FIG. 7. Plot of first order energy difference $\Delta E(n)$ [see Eq. (3.2)] as a function of cluster size (n).

the first energy difference $\Delta E(n)$ shows no conspicuous peaks. This is in sharp contrast to silicon clusters¹⁷ where binding energy evolves nonmonotonically and some clusters are found to be more stable than others. Thus the nature of bonding between Si and SiO_2 clusters is different. Mulliken population analysis on the atomic site for each cluster shown in Fig. 6 indicates significant charge transfer from Si to O. The charge transfer is relatively insensitive to the cluster size. In particular, the charge on the atomic site is seen to saturate when the coordination of Si and O, namely 4 and 2, respectively, is satisfied in the cluster.

Table IV shows the variation of the vertical ionization potential and the HOMO-LUMO gap (Δ) of $(\text{SiO}_2)_n$ clusters as a function of size. Note that the ionization potentials of $(\text{SiO}_2)_n$ clusters are rather high and increase steadily till $n=5$. Unlike the binding energy, the ionization potential drops for $n=6$. Our results are consistent with the experimental observation that it becomes more and more difficult to ionize the clusters as the size increases.¹⁸ This observation suggests that the usual spectroscopy measurement may not be suitable to probe electronic structure of large SiO_2 clusters and one may have to make use of high energy sources such as synchrotron facility which are currently available for cluster study. The HOMO-LUMO gap, on the other hand, increases steadily with cluster size. This characteristic is very different from the metal clusters where the HOMO-LUMO gap varies nonmonotonically with cluster size, but in general, decreases with increasing size of the clusters.

It is interesting to compare the ionization potentials and HOMO-LUMO gaps of Si_nO_m clusters for a fixed n and

TABLE III. Binding energy (measured against dissociated atoms) for various clusters using GAUSSIAN 94 and DMOL software.

Clusters	Total binding energy (eV)		Binding energy/ SiO_2 unit (eV)	
	GAUSSIAN 94	DMOL	GAUSSIAN 94	DMOL
SiO_2	12.54	13.43	12.54	13.43
Si_2O_4	28.69	30.56	14.35	15.28
Si_3O_6	45.30	48.12	15.10	16.04
Si_4O_8	61.86	65.65	15.47	16.41
Si_5O_{10}	78.43		15.69	
Si_6O_{12}	94.99		15.83	

TABLE IV. Vertical ionization potential and HOMO-LUMO gap for various clusters using GAUSSIAN 94 code.

Clusters	Ionization potential (eV)	HOMO-LUMO gap (Δ) (eV)
SiO_2	12.13	3.82
Si_2O_4	11.19	3.87
Si_3O_6	13.71	4.21
Si_4O_8	14.91	4.30
Si_5O_{10}	16.08	4.39
Si_6O_{12}	14.53	4.43

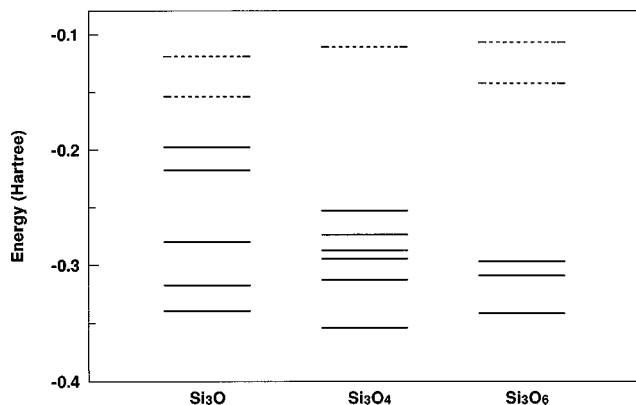


FIG. 8. Energy levels for Si_3O_m ($m=1,4,6$) clusters. Solid line indicates occupied orbitals while the dashed line indicates unoccupied orbitals. Only those energy levels close to the highest occupied molecular orbital (HOMO) and the lowest unoccupied molecular orbitals (LUMO) are given.

$m/n \leq 2$ in order to examine the role of oxygen defects on these properties. The data in Tables II and IV permit us to examine this for the Si_3O_m clusters. Recall that the ionization potential of Si_3O_6 is 11.02 eV, while that for Si_3O_4 and Si_3O are, respectively, 9.62 eV and 8.15 eV. Thus the ionization potential decreases with increasing oxygen defect concentration in silica clusters. These characteristics are also borne out in the HOMO-LUMO gap. In Fig. 8 we plot the molecular orbital energy levels of Si_3O , Si_3O_4 , and Si_3O_6 . The corresponding HOMO-LUMO gaps are 1.19 eV, 3.87 eV, and 4.21 eV. The fact that the HOMO-LUMO gap decreases in oxygen deficient silica clusters has important consequence for their optical properties. We had mentioned earlier that silica nanoparticles were observed to exhibit bright blue photoluminescence. Since the HOMO-LUMO gaps of $(\text{SiO}_2)_n$ particles ($n \leq 6$) (see Table IV) increase with size and are in the ultraviolet range, the blue emission could not arise simply because of the particle size. The origin for this emission must, therefore, be associated with defects. From the results in Fig. 8 and Table II, one can conclude that lack of oxygen in the silica nanoparticle could give rise to this interesting optical effect. We should remind the reader that the HOMO-LUMO gap in oxygen deficient Si_nO_m clusters will certainly depend on the Si content, i.e., the gap will change with particle size, n , even if m/n is fixed. It will be interesting to investigate this effect in larger oxygen deficient silica clusters.

IV. CONCLUSION

In summary, we have calculated the equilibrium geometries, energetics, and electronic structure of Si_nO_m clusters using the generalized gradient approximation (GGA) in the density functional theory. We note that our results agree very

well with available experimental data and theoretical calculations based on MP2 methodology. This establishes the validity of density functional approach in studying clusters that are bonded by strong covalent and/or partly ionic interaction. Our results, however, differ significantly from those obtained from molecular dynamics simulation based on an empirical pair potential. Although the bond lengths calculated using this potential agree reasonably with our results, the pair potential is unable to reproduce either the ground state or the relative stability of higher energy isomers correctly. We further note that the evolution of the atomic and electronic structure of silica clusters is very different from what is known in elemental semi-conductor and metallic clusters. While the bond distances and the nature of bonding vary little with cluster size, the ionization potentials and electron affinities not only depend on cluster size but also on their stoichiometric composition. For example, the ionization potentials and the HOMO-LUMO gap decrease with increasing oxygen deficiency. This could explain the novel optical properties of nanoscale silica particles. Further experimental and theoretical work on silica clusters with varying oxygen concentration would be very useful.

ACKNOWLEDGMENT

This work was supported in part by a grant from the Department of Energy (DEFG05-87E61316).

- ¹D. L. Helms, *Elements of Physical Geology* (Ronald, New York, 1969).
- ²G. W. Morey, *The Properties of Glass* (Reinhold, New York, 1954).
- ³E. Desurvire, *Phys. Today* **47**, 20 (1994).
- ⁴*The Physics and Chemistry of SiO₂ and Si-SiO₂ Interface*, edited by C. R. Helms and B. E. Deal (Plenum, New York, 1988).
- ⁵L. S. Wang, J. B. Nicholas, M. Dupuis, H. Wu, and S. D. Colson, *Phys. Rev. Lett.* **78**, 4450 (1997).
- ⁶S. Li, S. J. Silvers, and M. S. El-Shall, *J. Phys. Chem. B* **101**, 1794 (1997).
- ⁷J. A. Harkless, D. K. Stillinger, and F. H. Stillinger, *J. Phys. Chem.* **100**, 1098 (1996).
- ⁸L. Brus, *J. Phys. Chem.* **98**, 3575 (1994).
- ⁹J. Fan, J. B. Nicholas, J. M. Price, S. D. Colson, and L. S. Wang, *J. Am. Chem. Soc.* **117**, 5417 (1995).
- ¹⁰J. P. Perdew and Y. Wang, *Phys. Rev. B* **45**, 13 244 (1992).
- ¹¹A. D. Becke, *Phys. Rev. A* **38**, 3098 (1988).
- ¹²GAUSSIAN 94, Revision B.1, M. J. Frisch, G. W. Trucks, H. B. Schegel, P. M. W. Gill, B. G. Johnson, M. A. Robb, J. R. Cheeseman, T. Keith, G. A. Petersson, J. A. Montgomery, K. Raghavachari, M. A. Al-Laham, V. G. Zakrzewski, J. V. Ortiz, J. B. Foresman, J. Cioslowski, B. B. Stefanov, A. Nanayakkara, M. Challacombe, C. Y. Peng, P. Y. Ayala, W. Chen, M. W. Wong, J. L. Andres, E. S. Replogle, R. Gomperts, R. L. Martin, D. J. Fox, J. S. Binkley, D. J. Defrees, J. Baker, J. P. Stewart, M. Heads-Gordon, C. Gonzalez, and J. A. Pople (Gaussian, Inc., Pittsburgh, PA, 1995).
- ¹³DMOL code (Biosym Technologies Inc., San Diego, 1995).
- ¹⁴G. Herzberg, *Spectra of Diatomic Molecules* (Van Nostrand, New York, 1955).
- ¹⁵S. H. Vosko, L. Wilk, and M. Nusair, *Can. J. Phys.* **58**, 1200 (1980).
- ¹⁶S. Tsuneyuki, M. Tsukada, H. Aoki, and Y. Matsui, *Phys. Rev. Lett.* **61**, 869 (1988).
- ¹⁷M. F. Jarrold, *Science* **252**, 1085 (1991).
- ¹⁸L. S. Wang (private communication).